ISSN 1067-8212, Russian Journal of Non-Ferrous Metals, 2015, Vol. 56, No. 5, pp. 555–560. © Allerton Press, Inc., 2015.

POWDER MATERIALS AND COATINGS

Fluoridation of Hydroxyapatite with Addition of TiF_4 and Developing the Mechanical Properties by Pressureless Sintering[1]

Muhammad Asif[a, b, *], Zhengyi Fu[a], Muhammad Naveed Anjum[c], and Khalid Mahmood[b]

[a] *State Key Lab of Advanced Technology for Materials Synthesis and Processing, Wuhan University of Technology, Wuhan 430070, China*

[b] *Instituite of Chemical Sciences, Bahauddin Zakariya University, Multan, Pakistan*

[c] *Department of Applied and Biochemistry, Government College, University Faisalabad, Pakistan*

**e-mail: mhussain95@yahoo.com*

Abstract—Hydroxyapatite [$Ca_{10}(PO_4)_6(OH)_2$] powder was sintered with addition of aluminumisoproxide ($C_9H_{21}AlO_3$) 4 wt % and various wt % of titanium fluoride TiF_4. The prepared pellets were sintered at 1250°C temperature. The various wt % of TiF_4 were used for fluoridation and densification of hydroxyapatite. For studying the phase compositions, microstructure and elemental analysis, the sintered specimens were characterized by X-ray diffraction XRD, Scanning electron microscopy SEM, and energy dispersive electron spectroscopy EDAX respectively. After sintering highest relative density was found to be 96.42 % with Vickers hardness and bending strength 1.22–1.62 GPa and 13.39–35.88 MPa respectively. As a result of sintering fluoridated apatite composite material was obtained.

Keywords: fluoridation of hydroxyapatite, pressureless sintering, mechanical properties, fluoridated hydroxyapatite

DOI: 10.3103/S1067821215050028

1. INTRODUCTION

Hydroxyapatite HA [$Ca_{10}(PO_4)_6(OH)_2$] is a major mineralized phase of natural bone and teeth. Synthetic HA has been widely used in biomedical applications because of its bioactivity and biocompatibility [1, 2]. Synthetic HA has low fracture toughness which restricts its applications in load bearing implants [3]. Pure synthetic HA has problem of long term stability due to its high rate of bioresorption which results in loosening and failure of HA implants [3, 4]. Fluoridated hydroxyapatite F-HA has been used as a promising material in biomedical applications [5, 6]. It is found that the incorporation of fluoride ions into the HA structure considerably increases the resistance of HA against biodegradation and thermal decomposition [7]. In addition, fluoridated hydroxyapatite could provide better protein adsorption [8]. Moreover, fluoridated apatite shows better cell attachment than pure HA [9].

Cooper et al. and Guo et al. have used titanium copound with HA as durable bone implants [10, 11] and aluminum induces bone formation as they have mentioned [12]. Morover titanium oxide, titanium phosphate and aluminum phosphate have been used in other fields rather than orthopedics [13].

Fluorides study provides clear evidences that fluoride activates osteoblasts and improves the rate of minerals deposition in the body. Fluoride which exists in animal teeth and bones serves as essential element against dissolution [12]. So fluoridation and fluoridated hydroxyapatite (F-HA) has attracted many researchers attention as a promising material because F-HA shows significant resistance than pure HA against dissolution [14, 15]. Their work [14, 15] shows importance of fluoridation, densification and enhancing the mechanical properties. The use of TiF_4 with aluminumisoproxide and apatite is new research work. The aim of current research work is fluoridation, densification and developing the mechanical properties of hydroxyapatite composite material.

2. RAW MATERIALS AND EXPERIMENTAL PROCEDURES

Raw material was consisting of apatite, aluminumisopropoxide and TiF_4. Table 1 shows the various wt % of all five samples for clear understandings.

Five samples solution A, B, C, D and E were prepared in aqueous solution by using sol–gel technique. The sample solutions were stirred vigorously on magnetic stirrer at 70°C. After stirring sample solutions for 4 h, the solutions were aged for 12 h. Then suspension was filtered, washed with distilled water and ethyl alcohol for several times. Then powder was dried at 100°C for 12 h. Then obtained dry powder was designed into pellets, 20 mm in diameter. The pellets were sintered at 1250°C in gas tube furnace by using N_2 gas. The aim of using inert gas was to prevent the atmosphere oxygen to

[1] The article is published in the original.

Table 1. Concentrations of compounds to prepare samples (in wt %)

Sample	$C_9H_{21}AlO_3$	Apatite	TiF_4
A	4	91	5
B	4	87	9
C	4	83	13
D	4	80	16
E	4	77	19

react with sintering compounds. From room temperature to 900°C, the heating rate was 3°C/min and from 900°C to onward temperature, the heating rate was fixed 5°C/min. Each sample was sintered for holding time 1 h. The apparent porosity was fond by immersion the sintered pellets in distilled water. Bulk density of the sintered specimens was found by Archimedes rule. The phase composition of sintered samples was investigated by using X-ray diffraction (Rigaku Ultima II with Cu$K\alpha$ irradiation, Japan). To determine the chemical composition, the specimens were characterized by Energy Dispersive X-ray Spectroscopy EDX (Thermo Noran VANTAG-ESI). The sintered and polished specimens were cemented on copper stubs using graphite paint. Randomly various areas were chosen, observed and analyzed. Microstructures of sintered sample were observed by using Scanning Electron Microscopy SEM (Hitachi S-4800, Japan). For bending strength, the specimens were designed to bar shape of dimensions $3 \times 4 \times 25$ mm. The bending strength was measured in testing Centre of Wuhan University of Technology. The specimens were ground and polished for Vickers hardness. Hardness of the specimen was measured with Vickers indenter at load of 1 kg.

3. COMPOSITION AND PHASE TRANSFORMATIONS

The phase composition of sintered sample was studied by X-ray diffraction as shown in Fig. 1. The sintered samples were scanned at the scanning rate of 10°C/min at 2θ in the range from 10° to 80°. The resulted peaks were observed by their respective PDF cards numbers. Crystalline phases of compounds with their card numbers 75-2100–$CaTiO_3$, 76-0665–$(CaO)_{11}(Al_2O_3)_6$, 77-0120–$Ca_5(PO_4)_3F$, 87-2492–$(CaO)_{11}(Al_2O_3)_7CaF_2$ were identified. Major stronger peaks showing fluoridated apatite $Ca_5(PO_4)_3F$ was observed at 32°.

4. MICROSTRUCTURES

The SEM images of sintered samples are shown in Fig. 2. Grains size and grains boundaries are not very clear. It needs more research work. The effects of various sintering temperature on grains size will be studied in future research work. Micrograph of sample A

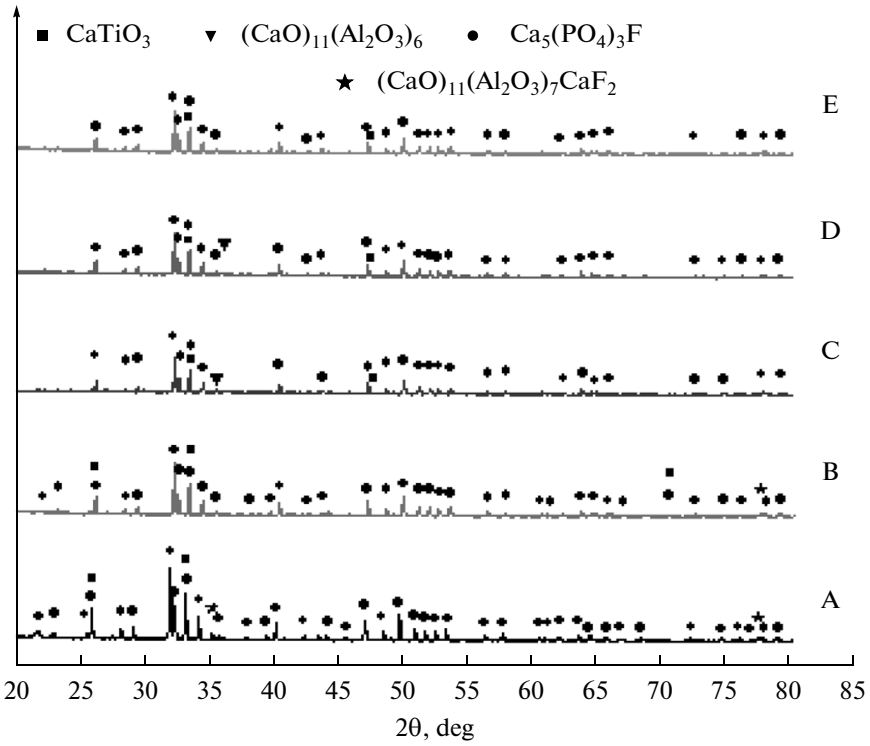

Fig. 1. X-ray diffraction pattern of samples A–E sintered at 1250°C for 1 h. (■) 75-2100–$CaTiO_3$, (▼) 76-0665–$(CaO)_{11}(Al_2O_3)_6$, (●) 77-0120–$Ca_5(PO_4)_3F$, (★) 87-2492–$(CaO)_{11}(Al_2O_3)_7CaF_2$.

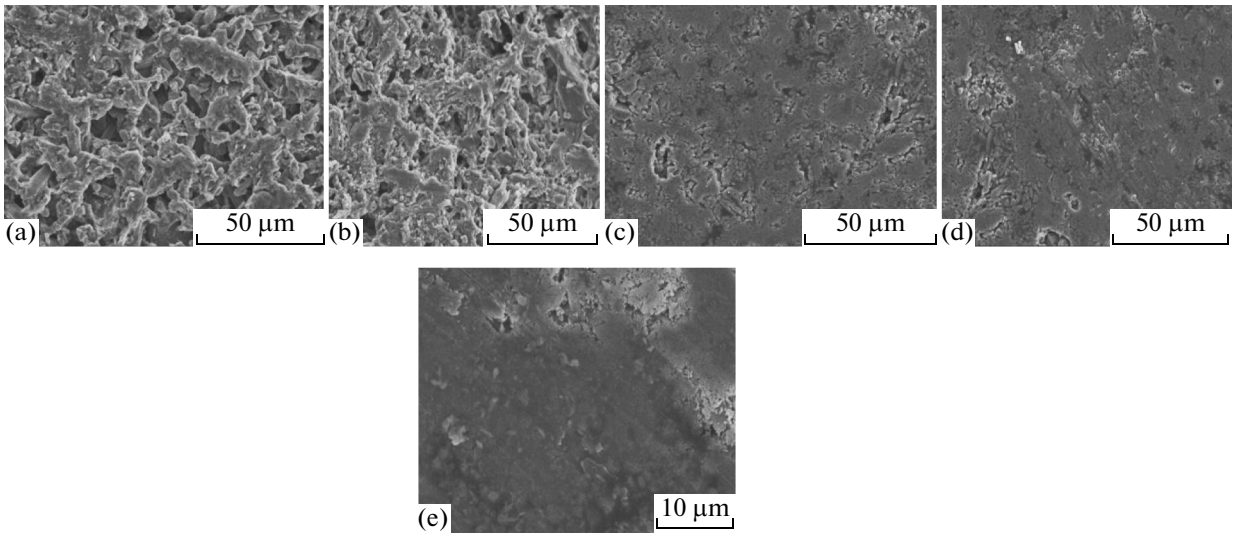

Fig. 2. Scanning electron microscopy SEM images of samples, A–E, sintered at 1250°C for 1 h.

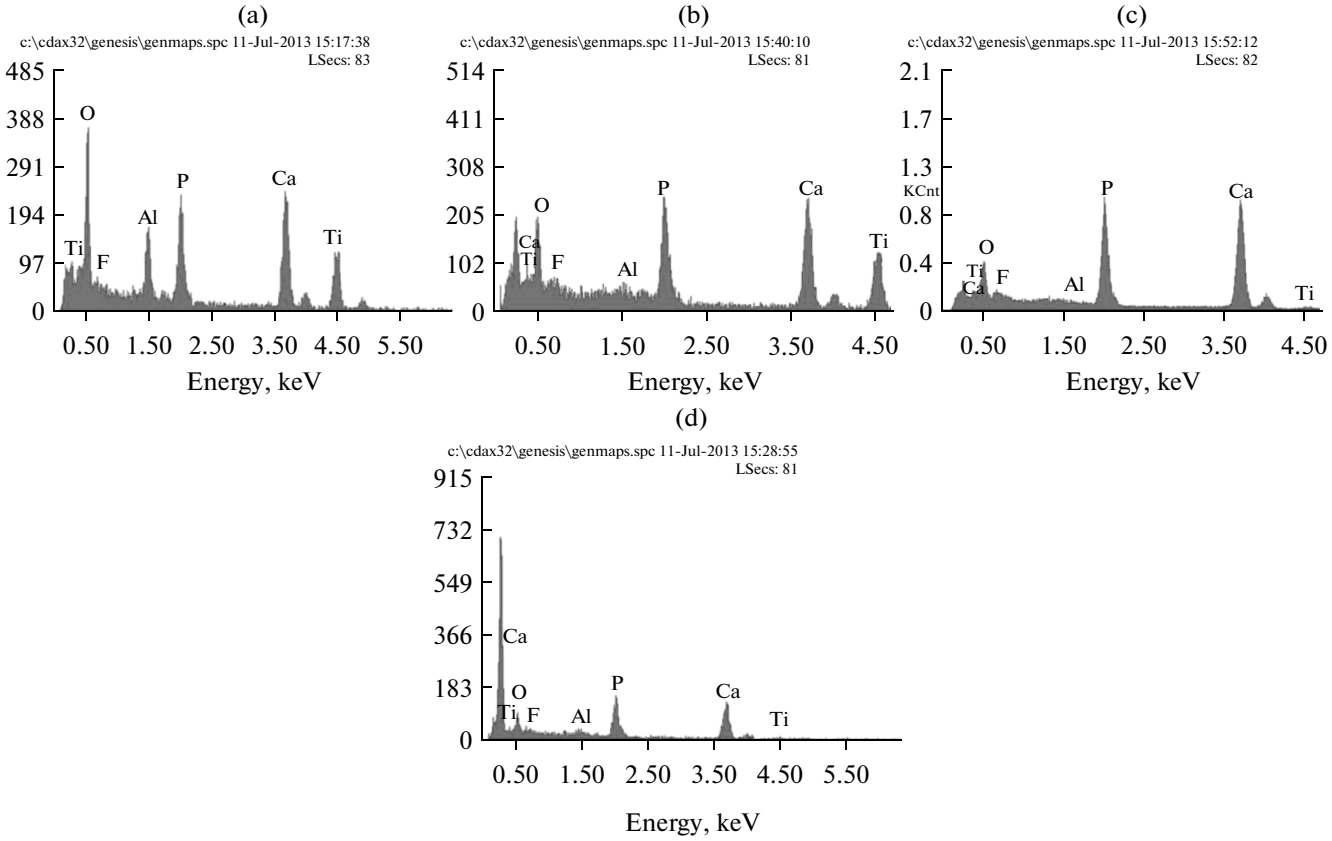

Fig. 3. EDS analysis of the samples A–E, sintered at 1250°C for 1 h.

shows the porosity and less densification. The sintered sample A has more pores and gaps among the particles while sample B has fewer pores. The sintered sample C and D have least porosity. Sample E has greatly densified as compare to sample C and D. Theses densities were calculated and confirmed by Archimedes rule.

5. ELEMENTAL ANALYSIS

Figure 3 shows a diffractogram of the samples sintered at 1250°C. Elements of sintered samples were analyzed by means of energy dispersive X-rays (EDAX). The various areas were observed randomly

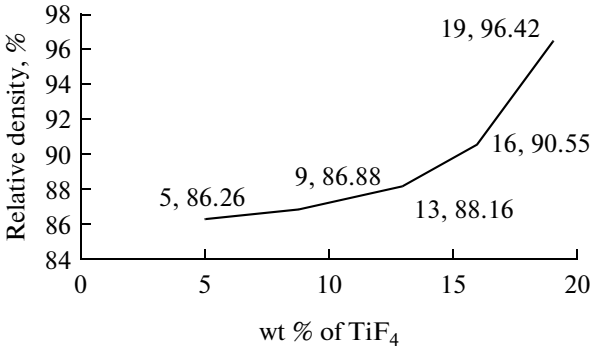

Fig. 4. Relationship of density vs. wt %-TiF_4 of samples A–E sintered at 1250°C.

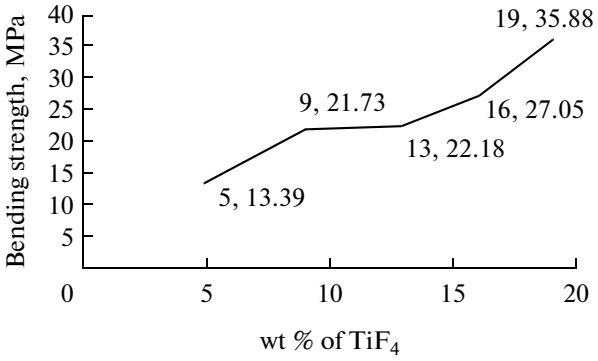

Fig. 6. Relationship of Bending strength vs. wt %-TiF_4 of samples A–E sintered at 1250°C.

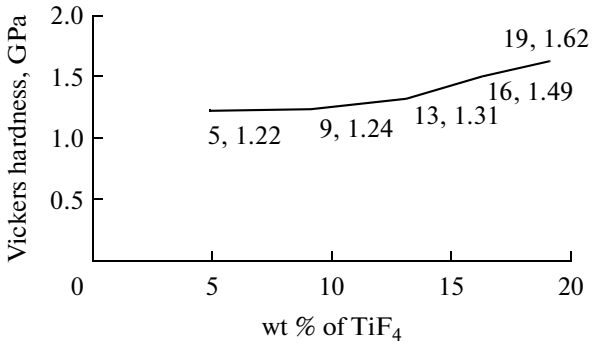

Fig. 5. Relationship of Vickers hardness vs. wt %-TiF_4 of samples A–E sintered at 1250°C.

on surface of sintered samples. The obtained peaks were labeled with their respective elements. The elements calcium, phosphorous, oxygen, aluminum, titanium and fluorine were identified in each sample. Phase composition XRD analysis has also confirmed that these elements are found in the sintered samples.

6. MECHANICAL PROPERTIES vs. wt % OF TiF_4

Figure 4 shows the relationship between density and various wt % of TiF_4. The graphical line shows that increasing the wt % of titanium fluoride TiF_4 density of samples has been increased. With addition of 19 wt %-TiF_4 the highest density of sintered sample E was found to be 96.4 %. Ramesh. et al. prepared apatite by various ways and sintered at maximum temperature 1400°C [16]. The relative density of our sintered apatite composite material has been found very close to their purely sintered apatite [16].

The changes in densification behavior and microstructure evolution greatly effects on mechanical properties of HA composites material. When the mechanical properties were studied, it was found that by increasing the wt % of TiF_4 Vickers hardness were also increased as has been explained in Fig. 5. The highest value of Vickers hardness of sample E was found to be 1.62 GPa. Increase in Vickers hardness are the functions of gradually increasing the addition of wt % of TiF_4 to the HA.

Figure 6 shows the relationship between bending strength and various wt % of TiF_4 added to the samples A–E. As graphical line shows that by increasing the wt % of TiF_4 the bending strength has been also

Table 2. Weight concentrations of $C_9H_{21}AlO_3$ and TiF_4 with their bending strength (in wt %), Vickers hardness, and relative densities

Sample	$C_9H_{21}AlO_3$, wt %	TiF_4, wt %	Bending strength, MPa	Vickers hardness, GPa	Relative density, %
A	4	5	13.39	1.22	86.26
B	4	9	21.73	1.24	86.88
C	4	13	22.18	1.31	88.16
D	4	16	27.05	1.49	90.55
E	4	19	35.88	1.62	96.42

increased. The maximum bending strength of sample E with addition of 19 wt % of TiF_4 was found to be 35.88 MPa. Monmaturapoj, et al. [17] studied the effect of sintering on microstructure and properties of hydroxyapatite produced by different synthesizing methods sintering at 1250°C. The bending strength of our fluoridated apatite composite material sintered at same temperature has been found greater than bending strength of apatite that was reported by Monmaturapoj et al.

7. CHEMICAL REACTIONS PROCESS

Expected chemical reactions are following

$$x\mathrm{Ca_{10}(PO_4)_6(OH)_2} + x[\mathrm{TiF_4}] + x\mathrm{H_2O} \rightarrow x\mathrm{Ca_{10}(PO_4)_6F_2} + x[\mathrm{TiF_3}]$$

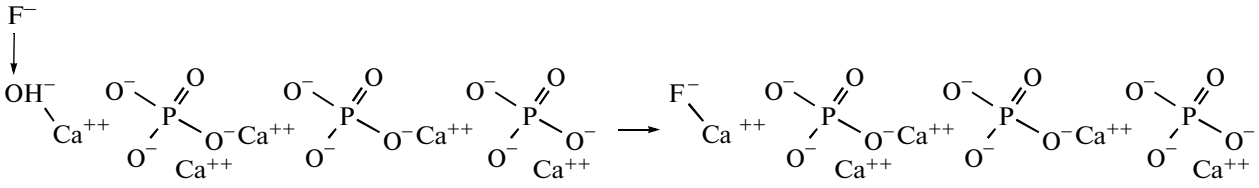

Tarasevich et al. [18] studied the modification of hydroxyapatite by substituting transition elements. This modification and change in composition is possible because there are three sites of apatite that can be substituted by other elements, i.e., Zn, F, Sr, Mg, etc., as they have reported also [19, 20]. These sites of apatite are Ca^{2+}, PO_4^{3-} and OH^-.

Fluoride ion is more electronegative than hydroxide ion and the size of the fluoride ion 1.32 Å is smaller than the size of hydroxide ion 1.68 Å. Fluoride ions can easily displace hydroxyl group of apatite.

In this work titanium fluoride has provided fluoride to apatite. As a result of sintering fluoridated hydroxyapatite has been obtained. Aluminumisopropoxide has decomposed into carbon dioxide and aluminum oxide. Aluminum oxide has reacted with calcium oxide and formed complex compound of calcium oxide and aluminum oxide. Titanium has reacted with calcium oxide and developed into calcium titanium oxide. Chemical equations have been explained on the basis of XRD results.

8. CONCLUSIONS

The addition of different wt % TiF_4 and $C_9H_{21}AlO_3$ to HA has improved mechanical properties. From the obtained results it has revealed that after sintering, bending strength and Vickers hardness have been improved with improving the densification. With addition of 19 wt % TiF_4, after sintering the sample, the highest Vickers hardness and bending strength has been found to be 35.88 Mpa and 1.62 GPa. While the highest vales of relative density of sintered sample has been found to be 96.42 %. As a result of sintering fluoridated hydroxyapatite composite materials has obtained.

REFERENCES

1. Boskey, A.L., Wnek, G., and Bowlin, G., Organic and inorganic matrices, *Encyclopedia of Biomaterials and Biomedical Engineering*, N.Y.: Informa Health Care, 2008, pp. 2039–2053.
2. Kim, H.M., Himeno, T., Kokubo, T., and Nakamura, T., Process and kinetics of bone like apatite formation on sintered hydroxyapatite in a simulated body fluid, *J. Biomater.*, 2005, vol. 26, pp. 4366–4373.
3. Mazaheri, M., Haghighatzadeh, M., Zahedi, A.M., and Sadrnezhaad, S.K., Effect of a novel sintering process on mechanical properties of hydroxyapatite ceramics, *J. Alloys Compounds*, 2009, vol. 471, pp. 180–184.
4. Darimont, G.L., Gilbert, B., and Cloots, R., Non-destructive evaluation of crystallinity and chemical composition by Raman spectroscopy in hydroxyapatite-coated implants, *J. Mater. Lett.*, 2003, vol. 58, no. 58, pp. 71–83.
5. Kim, H.W., Li, L.H., Koh, Y.H., Knowles, J.C., and Kim, H.E., Sol–gel preparation and properties of fluoride-substituted hydroxyapatite powders, *J. Am. Ceram. Soc.*, 2004, vol. 87, pp. 1939–1944.
6. Fathi, M.H. and Mohammadi Zahrani, E., Mechanical alloying synthesis and bioactivity evaluation of nanocrystalline fluoridated hydroxyapatite, *J. Cryst. Growth*, 2009, vol. 311, pp. 1392–1403.
7. Fathi, M.H., Mohammadi Zahrani, E., and Zomorodian, A., Novel luorapatite/niobium composite coating for metallic human body implants, *J. Mater. Lett.*, 2009, vol. 63, pp. 1195–1198.
8. Zeng, H., Chittur, K.K., and Lacefield, W.R., Analysis of bovine serum albumin adsorption on calcium phosphate and titanium surfaces, *Biomaterials*, 1999, vol. 20, no. 4, pp. 377–384.
9. Kim, H.W., Kong, Y.M., Bae, C.J., Noh, Y.J., and Kim, H.E., Sol-gel derived fluor-hydroxyapatite biocoatings on Zirconia substrate, *J. Biomater.,* 2004, vol. 25, pp. 2919–2926.
10. Cooper, L.F., Zhou, Y., and Takebe, J., Fluoride modification effects on osteoblasts behavior and bone for-

mation at TiO_2 grit-blasted c.p. titanium endosseous implants, *J. Biomater.*, 2006, vol. 27, pp. 926–936.

11. Guo, J., Padilla, R.J., Ambrose, W., De Kok, I.J., and Cooper, L.F., The effect of hydrofluoric acid treatment of TiO_2 grit blasted titanium implants on adherent osteoblasts gene expression in vitro and in vivo, *J. Biomater.*, 2007, vol. 28, pp. 5418–5425.
12. Aaseth, J., Boivin, G., and Andersen, O., Osteoporosis and trace elements—An overview, *J. Trace Elements Med. Biol.*, 2012, vol. 26, pp. 149–152.
13. Krut, E.N., Ko, et al., Heterogeneous composite of titanium oxide photocatalysts on phosphate support, *J. Theor. Exp. Chem.*, 2009, vol. 45, no. 1.
14. Barinov, S.M., Rustichelli, F., Orlovskii, V.P., Lodini, A., Oscarsson, S., and Firstov, S.A., Influence of fluoroapatite minor additions on behavior of hydroxyapatite ceramics, *J Mater. Sci.-Mater., Ser. M*, 2004, vol. 15, pp. 291–296.
15. Cheng, K., Weng, W.J., Qu, H.B., Du P.Y., Shen, G., Han, and G.R., Sol-gel preparation and *in vitro* test of fluorapatite/hydroxyapatite films, *J. Biomed. Mater. Res.*, 2004, vol. 69, pp. 33–37.
16. Ramesh, S., Aw, K.L., Tolouei, R., et al., Sintering properties of hydroxyapatite powders prepared using different methods, *J. Ceram. Int.,* 2013, vol. 39, no. 1, pp. 111–119.
17. Monmaturapoj, N. and Yatongchai, C., Effect of Sintering on microstructure and properties of hydroxyapatite produced by different synthesizing methods, *J. Met., Mater. Minerals*, 2010, vol. 20, no. 2, pp. 53–61.
18. Tarasevich, Yu.I., Vysotskaya, E.V., et al., IR spectroscopic study of the interaction of transition metal ions with hydroxyapatite modification by potassium ferrocyanide, *J. Theor. Exp. Chem.*, 2003, vol. 39, no. 5.
19. Ito, A., Otsuka, M., Kawamura, H., et al., Zinc-containing tricalcium phosphate and related materials for promoting bone formation, *J. Curr. Appl. Phys.*, 2005, vol. 5, no. 5, pp. 402–406.
20. Ito, A., Kawamura, H., Otsuka, M., et al., Zinc-releasing calcium phosphate for stimulating bone formation, *J. Mater. Sci. Eng., Ser. C,* 2002, vol. 22, no. 1, pp. 21–25.